2D/3D Discrete Duality Finite Volume Scheme (DDFV) applied to ECG simulation

A DDFV scheme for anisotropic and heterogeneous elliptic equations, application to a bio-mathematics problem: electrocardiogram simulation.

Yves COUDIÈRE* — **Charles PIERRE**** — **Olivier ROUSSEAU***** — **Rodolphe TURPAULT***

* Laboratoire de LMJL, UMR 6629 CNRS-UN-ECN. Université de Nantes, France.
{yves.coudiere,rodolphe.turpault}@univ-nantes.fr

** LMAP, UMR CNRS 5142. Université de Pau et des Pays de l'Adour, France.
charles.pierre@univ-pau.fr

*** Department of Mathematics and Statistics, University of Ottawa, Canada.
orous097@uottawa.ca

ABSTRACT. *This paper presents a 2D/3D finite volume (DDFV) method for solving heterogeneous and anisotropic elliptic equations on very general unstructured meshes. The derived approximation scheme is proved to be well-posed, symetric and positive definite, due to a discrete Green formulae. The method is used for the resolution of a problem arising in bio-mathematics: the ECG (electrocardiogram) simulation, on 2D and 3D meshes obtained from segmented medical images.*

KEYWORDS: *Anisotropic Heterogeneous Diffusion, Electrocardiology, 3D Discrete Duality Method*

1. Introduction

Based on the 2D DDFV method as defined e.g. in [DOM 05, AND 06], this paper introduces a new 3D finite volume discretisation for a linear elliptic equation. Consider a bounded domain $\Omega \subset \mathbb{R}^d$ ($d = 2, 3$), a conductivity tensor $G = G(x)$ (symmetric positive definite and uniformly elliptic on Ω) that is anisotropic and also heterogeneous and a function $f \in L^2(\Omega)$. We are looking for the variational solution ($\varphi \in H^1(\Omega)$) to

$$\text{div}(G\nabla\varphi) = f \text{ (in } \Omega), \quad G\nabla\varphi \cdot \mathbf{n} = 0 \text{ (on } \partial\Omega^N), \quad \varphi_{|\partial\Omega} = 0 \text{ (on } \partial\Omega^D), \quad (1)$$

where $\partial\Omega = \partial\Omega^N \cup \partial\Omega^D$, and $\mathbf{n}$ is a unit normal on the boundary of $\partial\Omega$. Specifically, in our model problem Ω is splitted into at least two parts, Ω_1 and Ω_2, and the tensor G is discontinuous along $\Gamma = \bar{\Omega}_1 \cap \bar{\Omega}_2$. When $G_{|\Omega_i}$ and Ω_i are smooth enough, the variational solution to (1) is in $H^2(\Omega_i)$ ($i = 1, 2$) and verifies

$$\varphi_{|\Omega_1} = \varphi_{|\Omega_2}, \quad G_{|\Omega_1} \nabla\varphi_{|\Omega_1} \cdot \mathbf{n} = G_{|\Omega_2} \nabla\varphi_{|\Omega_2} \cdot \mathbf{n} \quad \text{on } \Gamma. \tag{2}$$

Whenever $\partial\Omega^N = \partial\Omega$, uniqueness doesn't hold anymore and there is then a solution *iff* f has zero mean value, all solutions then differ up to a constant.

Our method provides a 3D symetric and positive-definite (main interest with respect to [HER 07]) finite volume method for this problem, that performs well on irregular meshes obtained from segmented medical images.

2. DDFV discretisation of the problem

2.1. *Mesh definition and discrete data*

We consider a triangulation/tetrahedrisation $\mathcal{C}$ of a bounded polygonal/polyhedral subset $\Omega \subset \mathbb{R}^d$. We denote by $\mathcal{V}$ and $\mathcal{I}$ the associated sets of vertices and interfaces (denoted by σ). The elements $C \in \mathcal{C}$ will be called *primal cells*. For equation (1) to be correctly discretised, we naturally assume that the mesh $\mathcal{C}$ "follows" the interface Γ, and that the boundary interfaces $\sigma \subset \partial\Omega$ are dealt into two subsets $\mathcal{I}^D$, $\mathcal{I}^N$ such that $\partial\Omega^N = \cup_{\sigma \in \mathcal{I}^N} \sigma$, $\partial\Omega^D = \cup_{\sigma \in \mathcal{I}^D} \sigma$. The set of vertices of the interfaces $\sigma \in \mathcal{I}^D$ is denoted by $\mathcal{V}^D \subset \mathcal{V}$. To every primal cell C is associated a centre $K \in C$ (its iso-barycentre in practice).

The cardinal of $\mathcal{C}$, $\mathcal{V}$, $\mathcal{V}^D$, $\mathcal{I}$ are denoted by $N_\mathcal{C}$, $N_\mathcal{V}$, $N_\mathcal{V}^D$, $N_\mathcal{I}$.

By C_K one denotes the primal cell C of centre K. To any interface $\sigma \in \mathcal{I}$ is associated a centre $Y_\sigma \in \sigma$ (also its iso-barycentre in practice), also simply denoted Y. Every internal interface $\sigma \in \mathcal{I}$ is the boundary between two primal cells C_1 and C_2. This is denoted by $\sigma = C_1 | C_2$. Any geometrical element (of dimension $0 < m \leq d$) has a positive m-dimensional measure denoted by $|\cdot|$ (like $|\sigma|$, $|C|$, $|\Omega|$, etc).

To every vertex $A \in \mathcal{V}$ is associated a *dual cell* P_A. Consider the subset $\mathcal{I}_A \subset \mathcal{I}$ of all the interfaces having A as a vertex. To every $\sigma \in \mathcal{I}_A$ is associated a geometrical element $P_{A,\sigma}$. The dual cell P_A is given by $P_A = \cup_{\sigma \in \mathcal{I}_A} P_{A,\sigma}$.

The elements $P_{A,\sigma}$ are defined as follows (see figure 1). Let $\sigma = C_K | C_L$ be an internal interface and let Y be σ's centre. In dimension 2, $P_{A,\sigma}$ is the quadrilateral $AKYL$. In dimension 3, let B and C be the two other vertices of σ ($\sigma = ABC$). Then $P_{A,\sigma}$ is the reunion of the two pyramids having the same quadrilateral base $ABYC$ and K, L for apex: $P_{A,\sigma} = ABYCK \cup ABYCL$. That definition has obvious extension to the case $\sigma \subset \partial\Omega$ (simply drop one of the pyramid).

REMARK. — In dimension 2 the (interiors of the) dual cells are disjoints and recover the whole domain, therefore $\sum_{A \in \mathcal{V}} |P_A| = |\Omega|$. Whereas in dimension 3 the dual
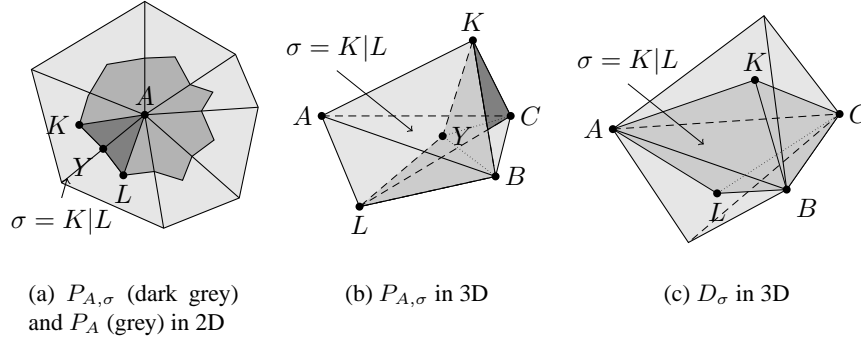
(a) $P_{A,\sigma}$ (dark grey) and P_A (grey) in 2D

(b) $P_{A,\sigma}$ in 3D

(c) D_σ in 3D

Figure 1. *Dual cells and Diamond cells*

cells are no more disjoints, if A and B are two vertices of the same interface σ, $P_{A,\sigma} \cap P_{B,\sigma} \neq \emptyset$. Actually the dual cells now recover exactly twice the whole domain, so that $\sum_{A \in \mathcal{V}} |P_A| = 2|\Omega|$.

To every interface $\sigma \in \mathcal{I}$ is associated one *diamond cell* D_σ. For an internal interface $\sigma = C_K | C_L$, it is defined as $D_\sigma = D_{\sigma,K} \cup D_{\sigma,L}$ where $D_{\sigma,K}$, $D_{\sigma,L}$ are the two triangles/pyramids with base σ and apex K and L respectively, as depicted on figure 1. In the case of a boundary interface $\sigma \subset \partial\Omega$, D_σ is a simple triangle/pyramid, $D_\sigma = D_{\sigma,K}$. The $D_{\sigma,K}$ will be called sub-diamond cells.

Hence the DDFV unknows belongs to the space $\mathbf{X}_h = \mathbb{R}^{N_C} \times \mathbb{R}^{N_{\mathcal{V}}}$. Its elements $\phi_h = ((\phi_K)_{K \in \mathcal{C}}, (\phi_A)_{A \in \mathcal{V}})$ are used to define pairs of piecewise constant functions $\phi_h = (\phi_h^{\mathcal{C}}, \phi_h^{\mathcal{V}})$ with $\phi_h^{\mathcal{C}}(x) = \sum_{K \in \mathcal{C}} \phi_K \mathbf{1}_{C_K}(x)$ and $\phi_h^{\mathcal{V}}(x) = \sum_{A \in \mathcal{V}} \phi_A \mathbf{1}_{P_A}(x)$ ($\mathbf{1}_X$ is caracteristic function of a subset $X \subset \Omega$).

The discret gradient of the DDFV unknown functions is defined on each side $(D_{\sigma,K}, D_{\sigma,L})$ of a diamond cell, and then belongs to the space $\mathbf{Q}_h = (\mathbb{R}^2)^{(d+1)N_C}$. Its elements are $q_h = (q_{\sigma,K})_{K \in \mathcal{C}, \sigma \in \delta K}$ with each $q_{\sigma,K}$ in $\mathbb{R}^2$. They also define piecewise constant vector valued functions $q_h(x) = \sum_{K \in \mathcal{C}} \sum_{\sigma \in \delta K} q_{\sigma,K} \mathbf{1}_{D_{\sigma,K}}(x)$.

The vector spaces $\mathbf{Q}_h$ and $\mathbf{X}_h$ are equipped with the inner products

$$(p_h, q_h)_{\mathbf{Q}_h} = \int_\Omega p_h(x) \cdot q_h(x) dx = \sum_K \sum_{\sigma \in \delta K} p_{\sigma,K} \cdot q_{\sigma,K} |D_{\sigma,K}|, \quad (3)$$

$$(\phi_h, \psi_h)_{\mathbf{X}_h} = \frac{1}{d} \left(\int_\Omega \phi_h^{\mathcal{C}}(x) \psi_h^{\mathcal{C}}(x) dx + \int_\Omega \phi_h^{\mathcal{V}}(x) \psi_h^{\mathcal{V}}(x) dx \right) \quad (4)$$

$$= \frac{1}{d} \left(\sum_K \phi_K \psi_K |K| + \sum_A \phi_A \psi_A |P_A| \right) \quad (5)$$

for $p_h, q_h \in \mathbf{Q}_h$ and $\phi_h, \psi_h \in \mathbf{X}_h$. The scaling $1/d$ appears because $\sum_K |K| = |\Omega|$ and $\sum_A |P_A| = (d-1)|\Omega|$ as seen before.

Now, consider a discrete diffusion tensor, piecewise constant on the half diamond cells $D_{\sigma,K}$, denoted by $G_h = (G_{\sigma,K})_{K \in \mathcal{C}, \sigma \in \delta K}$. We define the space $\mathbf{Q}_h^{(C)}$ as the subspace of the elements $q_h \in \mathbf{Q}_h$ that verify the *conservativity condition*

$$\forall \sigma \in \mathcal{I} \text{ such that } \sigma = C_K | C_L, \qquad G_{\sigma,K} q_{\sigma,K} \cdot \mathbf{n}_\sigma = G_{\sigma,L} q_{\sigma,L} \cdot \mathbf{n}_\sigma, \qquad (6)$$

$$\forall \sigma \in \mathcal{I}^N, \qquad G_{\sigma,K} q_{\sigma,K} \cdot \mathbf{n}_\sigma = 0. \qquad (7)$$

REMARK. — In the above definitions, there are one to one cannonical mappings from the spaces $\mathbf{Q}_\mathcal{C}$ and $\mathbf{X}_\mathcal{C}$ describing *degrees of freedom* (DOF) and the functions spaces of q_h and ϕ_h, so that the same notations can be used for vectors of DOF and functions. The DDFV formulation is based on the two finite volumes schemes on the primal and dual cells, with unknowns $\phi_h^\mathcal{C}$ and $\phi_h^\mathcal{V}$. The systems of equations on $\phi_h^\mathcal{C}$ and $\phi_h^\mathcal{V}$ are globally coupled through the calculation of the fluxes that are based on gradient functions in $\mathbf{Q}_h^{(C)}$ depending on both unknowns. The two systems decouples iff the mesh $\mathcal{C}$ is *admissible* as stated in [EYM 00]. Although this formulation uses some notations from the mimetic finite differences method (MFD), the scheme presented here doesn't belong to the category of MFD, for instance as analysed in [BRE 05].

2.2. *The discrete operators and the Green formulae*

The *discrete divergence* div_h is a linear mapping from $\mathbf{Q}_h^{(C)}$ to $\mathbf{X}_h$ defined for $q_h = (q_{\sigma,K})_{K \in \mathcal{C}, \sigma \in \delta K}$ by $\mathrm{div}_h q_h = ((\mathrm{div}_K q_h)_{K \in \mathcal{C}}, (\mathrm{div}_A q_h)_{A \in \mathcal{V}})$ with

$$\mathrm{div}_K q_h = \frac{1}{|C_K|} \int_{\partial C_K} q_h(x) \cdot \mathbf{n}_{\partial C_K} ds(x), \qquad (8)$$

$$\mathrm{div}_A q_h = \frac{1}{|P_A|} \int_{\partial P_A} q_h(x) \cdot \mathbf{n}_{\partial P_A} d(x), \qquad (9)$$

where $\mathbf{n}_{\partial E}$ is the outward unit normal on the boundary of the polygonal/polyhedral element E. That definition makes sense because of the conservativity condition (6).

The *discrete gradient* ∇_h must be defined in view of the conservativity condition (6). Therefore, auxiliary variables $(\phi_{Y_\sigma})_{\sigma \in \mathcal{I} \setminus \mathcal{I}^D}$ (to be defined by (6), (7)) are used, together with Dirichlet boundary values $(\phi_{Y_\sigma})_{\sigma \in \mathcal{I}^D} = 0$. Using these variables, the *discrete gradient* ∇_h is the linear mapping from $\mathbf{X}_h$ to $\mathbf{Q}_h^{(C)}$ defined for $\phi_h = ((\phi_K)_K, (\phi_A)_A)$ by $\nabla_h \phi_h = (\nabla_{\sigma,K} \phi_h)_{K \in \mathcal{C}, \sigma \in \delta K}$ with

$$\nabla_{\sigma,K} \phi_h = \frac{1}{|D_{\sigma,K}|} \int_{D_{\sigma,K}} \nabla \phi_{\sigma,K}^{(P1)}(x) dx, \qquad (10)$$

where $\phi_{\sigma,K}^{(P1)}$ is the function piecewise affine and continuous uniquely defined on $D_{\sigma,K}$ by its vertex values ϕ_K, ϕ_A, ϕ_B (and ϕ_C in 3D) and ϕ_Y using the triangulation (tetrahedridation in 3D) given by AKY and BKY ($ABKY$, $BCKY$, $CAKY$ in 3D – $\sigma = ABC$).

Proposition 2.1 *Given $K \in \mathcal{C}$ and $\sigma \in \delta K$, for $d = 3$ (assuming that $\sigma = ABC$ such that $\det(B - A, C - A, x_K - A) > 0$) consider $N_{\sigma K} = \frac{1}{2}(B - A) \wedge (C - A)$, $N_A = \frac{1}{2}(Y - A) \wedge (x_K - Y)$, $N_B = \frac{1}{2}(Y - B) \wedge (x_K - B)$, $N_C = \frac{1}{2}(Y - C) \wedge (x_K - C)$; then we have*

$$\nabla_{\sigma,K}\phi = \frac{1}{3}\frac{1}{|D_{\sigma,K}|}\left((\phi_K - \phi_Y)N_{\sigma K} + (\phi_B - \phi_C)N_A \right.$$

$$\left. + (\phi_C - \phi_A)N_B + (\phi_A - \phi_B)N_A\right).$$

If $d = 2$, and with $N_{\sigma K} = (B - A)^\perp$, $N_{AB} = (x_K - Y)^\perp$ ($\cdot^\perp$ denotes the rotation of angle $+\pi/2$), with $\sigma = AB$ such that $\det(B - A, x_K - A) > 0$, we have

$$\nabla_{\sigma,K}\phi = \frac{1}{2}\frac{1}{|D_{\sigma,K}|}\left((\phi_K - \phi_Y)N_{\sigma K} + (\phi_B - \phi_A)N_{AB}\right).$$

Proof. This is a simple computation (see figure 1 for the notations). ∎
REMARK. — In proposition 2.1 the values of ϕ_Y can be easily expressed in terms of only $\phi_K, \phi_A, \phi_B, \phi_C$ as solutions to the scalar equations (6) or (7).

The previously defined discrete operators fulfil a duality property called *discrete Green formula* by analogy with the continuous case.

Proposition 2.2 *Consider a discrete tensor $G_h = (G_{\sigma,K})_{K \in \mathcal{C}, \sigma \in \delta K}$. For any $\phi_h \in \mathbf{X}_h$ such that $\phi_A = 0$ for all $A \in \mathcal{V}^D$ and $q_h \in \mathbf{Q}_h^{(C)}$, we have*

$$(div_h q_h, \phi_h)_{\mathbf{X}_h} + (q_h, \nabla_h \phi_h)_{\mathbf{Q}_h} = 0. \tag{11}$$

Proof. It is a straightforward computation based on proposition 2.1 and on (3)-(9). ∎
REMARK. — A similar equality holds in the general non homogeneous case, with boundary terms on the right hand side, assuming the discretisation accounts for the boundary conditions.

2.3. *The problem discretisation*

Once the diffusion tensor $G(x)$ has been discretized, for instance with

$$\forall K \in \mathcal{C}, \ \forall \sigma \in \delta K, \quad G_{\sigma,K} = \frac{1}{|D_{\sigma,K}|}\int_{D_{\sigma,K}} G(x)dx,$$

solving (1) with the DDFV finite volume method consist in looking for the unknown $\phi_h = (\phi_h^{\mathcal{C}}, \phi_h^{\mathcal{V}}) \in X_h$ such that $\phi_A = 0$ for any $A \in \mathcal{V}^D$ and

$$-div_h G_h \nabla_h \phi_h = f_h \quad \text{in } \mathbf{X}_h, \tag{12}$$

with $f_h = ((f_K)_K, (f_A)_A) \in \mathbf{X}_h$ defined by

$$\forall K \in \mathcal{C}, \; f_K = \frac{1}{|C_K|} \int_{C_K} f(x)dx, \quad \forall A \in \mathcal{V}, \; f_A = \frac{1}{|P_A|} \int_{P_A} f(x)dx. \quad (13)$$

REMARK. — From (8), (9) and (13), it can be seen that (12) is a discretisation of the integral equation $-\int_{\partial V} G \nabla \phi \cdot \mathbf{n}_V \, d\sigma = \int_V f$ on the finite volumes $V = K$ or A, using fluxes based on the gradient $\nabla_h \phi_h \in \mathbf{Q}_h^{(C)}$ that are *conservative with respect to* G_h as expressed by (6).
Equation (12) is a linear system of $N_{\mathcal{C}} + N_{\mathcal{V}} - N_{\mathcal{V}}^D$ equations with $N_{\mathcal{C}} + N_{\mathcal{V}} - N_{\mathcal{V}}^D$ unknowns. As a consequence of proposition 2.2 we have the

Proposition 2.3 *The linear system* (12) *is symetric and positive with respect to the scalar product* $(\cdot, \cdot)_{\mathbf{X}_h}$:

$$(-div_h G_h \nabla_h \phi_h, \phi_h)_{X_h} \geq \alpha \|\nabla_h \phi_h\|_{L^2(\Omega)}^2,$$

where $\alpha > 0$ is the constant of ellipticity of $G(x)$. The discrete problem has a unique solution if $\mathcal{I}^D \neq \emptyset$ (mixed Dirichlet and Neumann).

Proof. The proof is deduced from a reformulation of summations appearing in the inner products. ∎

3. Application

The bidomain model (see *e.g.* [KEE 98]) describes the electrical activity of the heart inside the Torso. In our application, the heart and torso are modeled by a 2D slice of a segmented MRI image (figure 2). The region separated by dark lines on figure 2(middle) are myocardium (domain H), ventricular cavities, lungs and torso (domain $T = \Omega \backslash H$). The model inside the myocardium involves two compartments: the intra/extra cellular mediums, and models a trans-membrane potential $v = \varphi_i - \varphi$, difference between the intra/extra cellular potentials respectively. The extracellular potential ϕ further extends inside the cavities and outside to the whole torso. At each time step, this extended potential is at electrostatic equilibrium. Its measure at the surface of the torso is the electrocardiograms (ECG).

For sake of simplicity, the *modified monodomain* model (see [CLE 04]) is used: $v(x,t)$ is given directly as the solution of a reaction diffusion system involving a second variable $\mathbf{w}(x,t) \in \mathbb{R}^m$ that describes the cells membrane activity (m is up to 20) using stiff differential equations. It is used to simulate the normal propagation of depolarization and repolarization wave fronts (v passing from a rest value to a plateau value and back to its rest value). It reads in H,

$$A_0 \left(C_0 \frac{\partial v}{\partial t} + I_{ion}(v, \mathbf{w}) \right) = \text{div}(G_1 \nabla v) + I_{app}(x,t), \quad \frac{\partial \mathbf{w}}{\partial t} = g(v, \mathbf{w}), \quad (14)$$

while the electrostatic balance equation on $\Omega = H \cup T$ is

$$-\operatorname{div}(G\nabla\phi(t)) = [\operatorname{div}(G_3\nabla v(t))]\,\mathbf{1}_H \tag{15}$$

The data A_0 and C_0 are constants scalars, the tensor $G_1 = G_1(x)$ is non constant and anisotropic, I_{ion}, g are reaction terms, I_{app} is an externally applied current that activates the system and in equation (15), $G = G(x)$ and $G_3 = G_3(x)$ are non constant tensors. The microscopic orientation of the muscle fibers inside the myocardium is
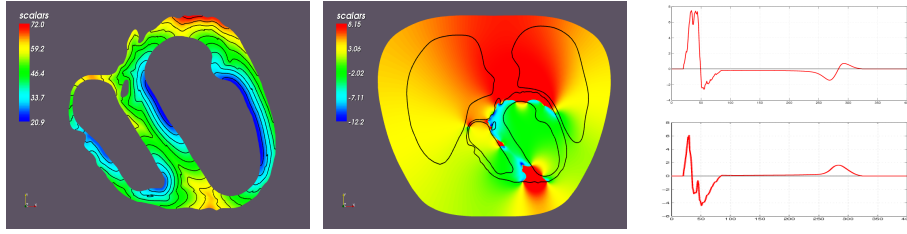

Figure 2. *(left) Simulation of v: isochrons (ms) for the excitation wave on a 2D ventricles slice mesh coming from MRI segmented images, 485000 degrees of freedom. (middle) Computation of φ at time $t = 50ms$. The four domains are separated with black lines (ventricles, ventricles cavities, lungs and torso remaining). (right) Simulated ECG for two leads (V1 and V2) located on the body surface.*

represented in the anisotropic diffusion tensors, $G_1(x)$ (in eq. (14)) and $G_2(x)$, $G_3(x)$ (in eq. (15)). They all have the form $G_i(x) = P^{-1}(x)D_iP(x)$ ($i = 1,2,3$) where D_i is diagonal, representing longitudinal and transverse conductivities, and $P(x)$ is a change of basis matrix from the Frenet basis attached to the fibre direction at point x.

At last, the global conductivity matrix $G = G(x)$ is used to take into account the difference of conductivity between the lungs, ventricular cavities, etc.

$$G(x) = \begin{cases} G_2(x) & \text{for } x \in H, \\ G_{\text{cavities}} & \text{in the ventricular cavities,} \\ G_{\text{lung}} & \text{in the lungs,} \\ G_0 & \text{otherwise.} \end{cases} \tag{16}$$

A homogeneous Neumann condition is attached to eq. (15) on the boundary $\partial\Omega$, to express that no current flow out of the torso.

Our main problem is to solve eq. (15), that is exactly of the form (1) with a discontinuous and anisotropic diffusion tensor $G(x)$ given in (16). The right-hand side is given by the solution to (14), previously computed using the DDFV method and explicit time-integration.

It is numerically difficult because a fine mesh and a small time step are needed to account for the dynamics of the reaction-diffusion system (14). Our segmented 2D

data counts 600 000 degrees of freedom (485 000 in H). Furthermore we solve an homogeneous Neumann problem and the discrete matrix for (15) is ill-conditionned. A GMRes solver with SSOR preconditionning has been found to perform reasonably for this problem. The potential ϕ is computed with a coarser time-step of 1 ms. On a whole cardiac cycle ($\simeq 600\ ms$), 600 computations (linear system solutions) are thus performed.

The 3D version of the code is in progress. Yet it is possible to perform 3D simulations considering only the isolated heart. The example given below shows the evolution of V_m inside the ventricles on a 49611 thetrahedra mesh, as computed by the 3D DDFV method.
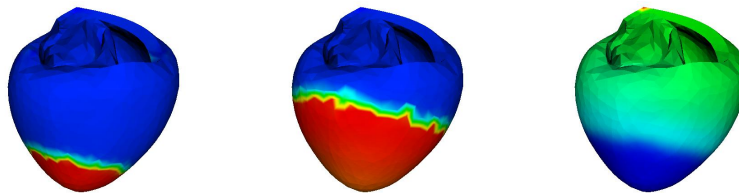

Figure 3. *Example of 3D computation (isolated heart) - Evolution of V_m.*

4. References

[AND 06] ANDREIANOV B., BOYER F., HUBERT F., "Discrete-duality finite volume schemes for Leray-Lions type elliptic problems on general 2D meshes", *Num. Methods for PDE*, vol. 23, num. 1, 2006, p. 145 - 195.

[BRE 05] BREZZI F., LIPNIKOV K., SHASHKOV M., "Convergence of Mimetic Finite Difference Method for Diffusion Problems on Polyhedral Meshes", *SIAM J. Numer. Anal.*, vol. 43, num. 5, 2005, p. 1872-1896.

[CLE 04] CLEMENTS J., NENONEN J., HORACEK M., "Activation Dynamics in Anisotropic Cardiac Tissue via Decoupling", *Annals of Biomed. Eng.*, vol. 32, num. 7, 2004, p. 984-990.

[DOM 05] DOMELEVO K., OMNÈS P., "A finite volume method for the Laplace operator on almost arbitrary two-dimensional grids", *M2AN*, vol. 39, num. 6, 2005, p. 1203-1249.

[EYM 00] EYMARD R., GALLOUËT T., HERBIN R., "*Solution of Equations in Rn (Part 3), Techniques of Scientific Computing (Part 3)*", vol. 7 of *Handbook of Numercial Analysis*, chapter Finite Volume Methods, North-Holland, 2000.

[HER 07] HERMELINE F., "Approximation of 2-D and 3-D diffusion operators with variable full tensor coefficients on arbitrary meshes", *Comput. Methods Appl. Mech. Eng.*, vol. 196, num. 1, 2007, p. 2497-2526.

[KEE 98] KEENER J., SNEYD J., *Mathematical Physiology*, Springer-Verlag, 1998.